Submicron aerosol size distributions and cloud condensation nuclei concentrations measured at Gosan, Korea, during the Atmospheric Brown Clouds–East Asian Regional Experiment 2005

Greg Roberts, Seong Soo Yum, Jong Hwan Kim, Keunyong Song, Dohyeong Kim

Submicron aerosol size distributions and cloud condensation nuclei concentrations measured at Gosan, Korea, during the Atmospheric Brown Clouds–East Asian Regional Experiment 2005

Seong Soo Yum,[1] Greg Roberts,[2] Jong Hwan Kim,[1] Keunyong Song,[1] and Dohyeong Kim[2]

Received 1 November 2006; revised 15 February 2007; accepted 14 March 2007; published 27 October 2007.

[1] Submicron aerosol size distributions, CN and CCN concentrations at a constant supersaturation of 0.6% were measured at a relatively remote coastal site at Gosan in Jeju Island, Korea, during the ABC-EAREX from 11 March to 8 April 2005. The average CN concentrations were 6088 ± 3988, 5231 ± 2454 and 3513 ± 1790 cm^{-3}, respectively, for the three major air mass types classified by their origins. The corresponding CCN concentrations were 2393 ± 1156, 2897 ± 1226 and 1843 ± 585 cm^{-3}. The type III air mass was the closest to maritime origins, but these lowest concentrations at Gosan were an order of magnitude higher than those of clean marine boundary layer, indicating that regardless of air mass designation springtime submicron aerosols at Gosan were under steady continental influences. Distinct new particle formation and growth events occurred on 6 d, when clear sky weather conditions prevailed that brought air from northern China, Mongolia or Russia by anticyclonic circulations. Simultaneous occurrence of these events at a western coastal site in the Korean Peninsula 350 km north of Gosan suggests that these events were not local but at least regional-scale events. CCN concentrations were predicted with the aerosol size distributions and the assumption of particles being composed of $(NH_4)_2SO_4$. The predicted to measured CCN concentration ratio was 1.27 ± 0.29 and the r^2 was 0.77 for the whole measurement period. The type I air mass that has the most continental influences showed a slight tendency to overpredict CCN concentrations but the good agreement overall suggests that springtime Gosan aerosols act almost like ammonium sulfate as far as CCN activity is concerned, almost regardless of air mass origin.

Citation: Yum, S. S., G. Roberts, J. H. Kim, K. Song, and D. Kim (2007), Submicron aerosol size distributions and cloud condensation nuclei concentrations measured at Gosan, Korea, during the Atmospheric Brown Clouds–East Asian Regional Experiment 2005, *J. Geophys. Res.*, *112*, D22S32, doi:10.1029/2006JD008212.

1. Introduction

[2] Submicron aerosols dominate the number concentration of atmospheric particles [*Hobbs*, 2000]. They encompass newly formed nanometer size particles by gas to particle conversion to large particles formed by coagulation of these small particles and gas condensation onto existing particles and also by cloud processing [e.g., *Hoppel et al.*, 1986]. Importantly a great majority of number concentrations of atmospheric particles of anthropogenic origin belong to this size category [*Seinfeld and Pandis*, 1998]. The concentrations and size distributions of submicron aerosols vary greatly with geographical locations and in one location they can also temporally vary with the local source activities and transport pathways determined by meteorology [*Jaenicke*, 1993]. So there is intrinsic variability of submicron aerosol distributions at any given location.

[3] Nevertheless atmospheric submicron aerosols have been of great interest. Since their sizes are comparable to solar wavelengths, visibility is directly affected. More importantly in a climatic sense, atmospheric particles of these sizes crucially affect the solar radiation budget directly by absorption and scattering [*Harshvardhan*, 1993]. Moreover cloud condensation nuclei (CCN) that can be activated to become cloud droplets at water supersaturations (S) of atmospheric clouds (<1%) are mostly of these sizes; for example $(NH_4)_2SO_4$ particles of 0.1% critical supersaturation (S_c) are 0.135 μm in diameter (D_p) [*Pruppacher and Klett*, 1997]. Since CCN concentration and composition are among the most important factors that determine cloud microphysical properties, which in turn determine cloud albedo and influence cloud lifetime and extent, solar

[1]Department of Atmospheric Sciences, Yonsei University, Seoul, South Korea.
[2]Center for Atmospheric Sciences, Scripps Institution of Oceanography, La Jolla, California, USA.

0148-0227/07/2006JD008212

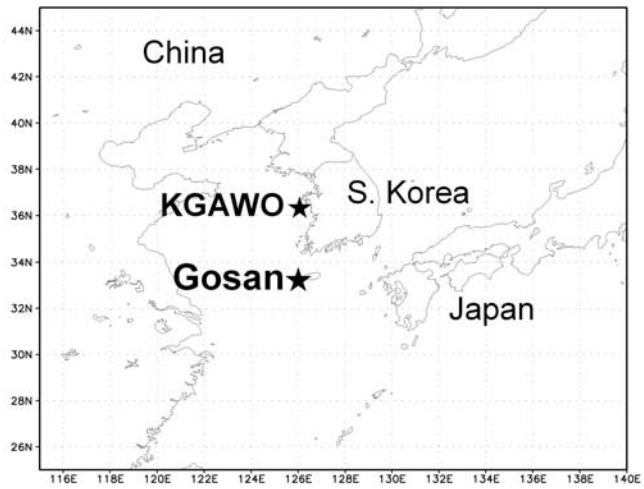

Figure 1. Map around the Gosan measurement site. The Korea Global Atmosphere Watch Observatory (KGAWO) is also marked for reference.

radiation budget is indirectly affected by aerosols acting as CCN [*Twomey*, 1977; *Albrecht*, 1989].

[4] There have been a number of field studies in the last two decades that aimed at improving our understanding of atmospheric aerosols and their role in climate prediction [e.g., *Ramanathan et al.*, 2001]. However, correct assessment of aerosol radiative forcing is still a formidable task because of the great spatial and temporal variability of atmospheric aerosol distributions and their optical and chemical properties. The aerosol indirect effects, which require proper understanding not only of what portion of aerosols can act as CCN but also of the atmospheric dynamics that determine cloud development, are considered to be the greatest source of uncertainties in climate prediction [*Intergovernmental Panel on Climate Change*, 2001].

[5] This study presents submicron aerosol size distributions, total particle (i.e., condensation nuclei, CN) concentrations (N_{CN}), and CCN concentrations (N_{CCN}) measured at a coastal site at Gosan in Jeju Island of Korea (Figure 1) during the Atmospheric Brown Clouds–East Asian Regional Experiment in 2005 (ABC-EAREX 2005), the purpose and scope of which are described in detail by T. Nakajima et al. (Overview of the ABC EAREX 2005 regional experiment and a study of the aerosol direct radiative forcing in east Asia, submitted to *Journal of Geophysical Research,* 2007). Fast economic growth and industrialization in China and other regions in East Asia necessarily designate the Gosan site as one of the key locations to monitor the influence of Asian continental outflow. This site was also used as a key ground measurement station during the Aerosol Characterization Experiment in Asia (ACE-Asia) conducted in April–May 2001 [*Huebert et al.*, 2003]. The main purpose of this study is to characterize springtime submicron aerosol size distributions and CN and CCN concentrations at this coastal site, on which only a few numbers of papers have been published in scientific journals [e.g., *Yum et al.*, 2005; *Adhikari et al.*, 2005]. An attempt is also made to link aerosol size distributions to CCN concentrations as an effort to predict CCN concentrations from aerosol size distributions [*Roberts et al.*, 2006]. Lacking in this study is the chemical characterization of submicron aerosols, which can be found elsewhere in this special issue.

2. Experiment

[6] Measurements were made in an instrument shelter at the Gosan site located on a cliff (~50 m ASL) at the western tip of the Jeju Island's coastline (Figure 1), which is reported to have the lowest local anthropogenic emission in Korea [*Kim et al.*, 1998]. The instrument shelter is located about 10 m inland from the cliff edge. The site and its surrounding areas are covered with grass. The agricultural activity at the village located 1 km to the east of the site is minor. Sample air was drawn from the 6 m stainless steel inlet pipe of 15 cm diameter vertically aligned through the ceiling of the instrument shelter and then delivered to different instruments from the manifold structured to be at 90° angle with the inlet pipe. Therefore the sample air came from approximately 8 m above the ground and 58 m above the sea surface, avoiding immediate influence of sea spray particles. The whole measurement period was from 11 March to 8 April 2005 but CCN measurements ended on 30 March.

[7] A Scanning Mobility Particle Sizer (TSI SMPS-3936L10) measured aerosol number size distributions ($10\ nm < D_p < 300\ nm$) every 3 min with a resolution of 65 channels per decade. The manufacture-provided data inversion program with the diffusion loss correction routine was applied. Integration of SMPS measured aerosol number distribution provides total particle concentration for the given size range (N_{SMPS}); to differentiate from N_{CN} measured by a Condensation Particle Counter (TSI CPC-3010; $D_p > 10\ nm$) with 1 min time resolution. Since TSI CPC-3010 model saturates at concentrations greater than $10^4\ cm^{-3}$ because of coincidence pulses, a sample air dilution system was introduced for this measurement and then measured concentrations were multiplied by the dilution factor to calculate actual concentrations. A stream-wise thermal gradient CCN counter [*Roberts and Nenes*, 2005] built at Scripps Institute of Oceanography measured N_{CCN} at a fixed S of 0.6% with a time resolution of 10 s.

[8] Aerosol size distributions, CN and CCN concentrations were continuously measured throughout the whole measurement period except occasional breaks of an hour or so for maintenance. There were no size distribution measurements on 27 March because of SMPS malfunctioning. CCN data were also continuous except some data had to be discarded since they were measured under improper conditions such as insufficient wetting of the column. On average CCN data were not available for 2.4 h in each CCN measurement day.

3. Results

3.1. Air Mass Designation

[9] Figure 2 shows all of the 6-hourly 3 d air mass back trajectories calculated by the HYSPLIT4 model [*Draxler and Hess*, 1998] for the entire measurement period, which have been classified into three major types. Type I air mass originated mostly from remote continental northern China,

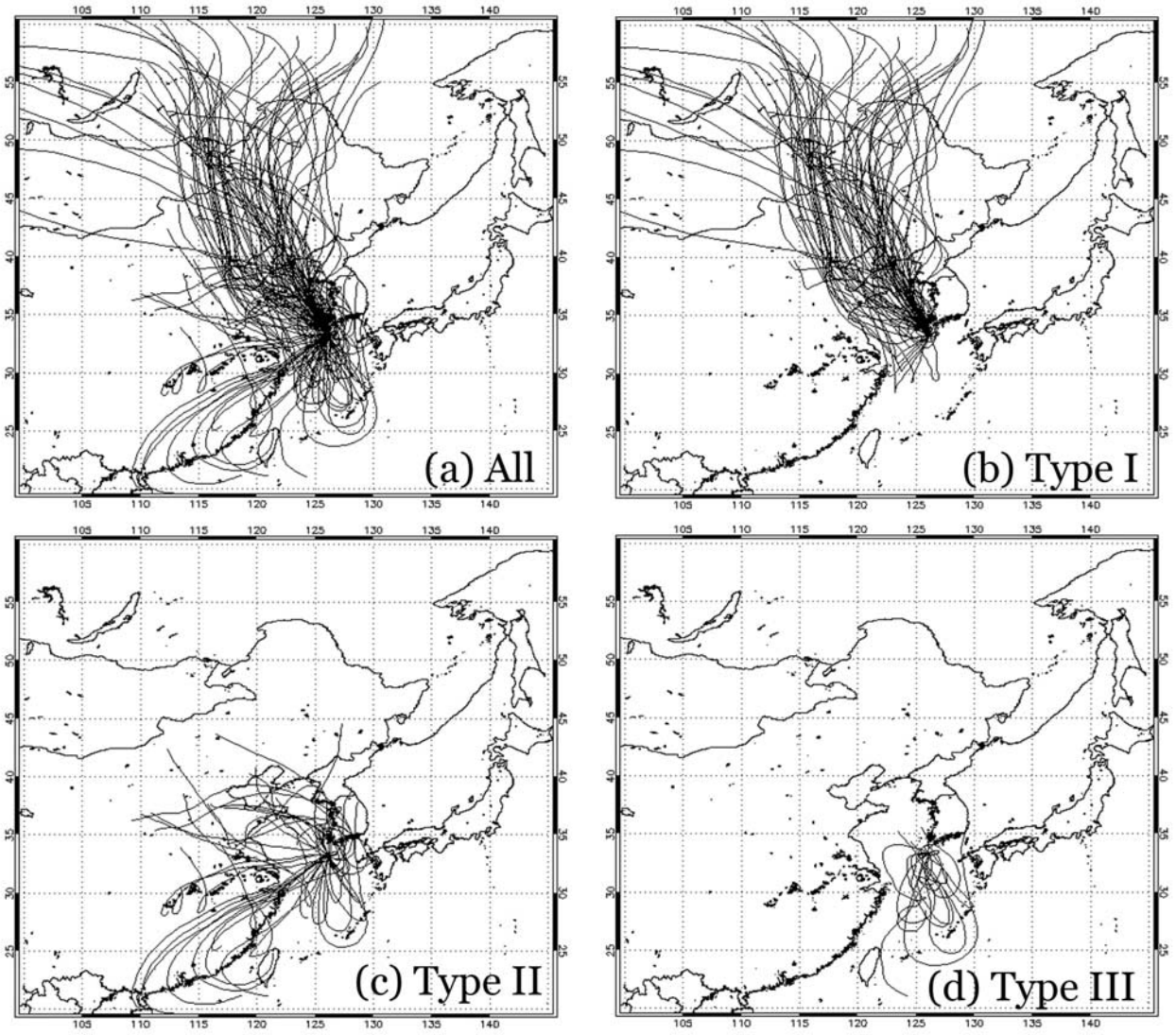

Figure 2. The 6-hourly air mass back trajectories from the Gosan measurement site (500 m ASL) for (a) the entire measurement period, (b) type I, (c) type II, and (d) type III air masses.

Mongolia or Russia and passed over the Yellow Sea before arriving at Gosan (Figure 2b). The weather patterns for these trajectories usually showed a solid high-pressure system centered in eastern China, generating northwesterly winds to the east by anticyclonic circulations. The weather at Gosan was mostly clear sky for these trajectories (Figure 3; more on this figure later). The origin of the type II air mass varied a lot but was close to coastal areas in China and Korea where the population density is high. Type II trajectories spent the majority of time over the Yellow Sea or the South China Sea before they arrived at Gosan (Figure 2c). Type III air mass originated over the sea and spent almost the entire time over the sea south of Jeju Island (Figure 2d). The weather patterns for type II and III usually showed a low-pressure system or a frontal system passing through Jeju Island and the weather was cloudy or rainy (Figure 3). Presumably type I may be classified as remote continental, type II anthropogenically modified maritime, and type III maritime but as it turns out, these classifications have only a trace of their typical characteristics and they may all be broadly classified as continental/polluted.

3.2. Aerosol Distributions

[10] The total and each air mass type averages of particle concentrations (N_{CN} and N_{SMPS}) and CCN concentration (N_{CCN}) are listed in Table 1 and the time series of the daily averages are shown in Figure 3. Different shadings in Figure 3 represent the air mass types. Also shown is the weather report (''clear sky'' or ''cloudy or rainy'') for each day by the ABC science team. The weather may have varied in the middle of the day and therefore this report is sort of an overall assessment. The days when particle formation and growth events occurred were marked on the top axis and will be discussed in more detail in the next subsection.

[11] The average N_{CN} and N_{SMPS} for the entire measurement period are 5599 ± 3518 cm^{-3} and 5337 ± 3427 cm^{-3}, respectively (Table 1). The less than 5% difference between

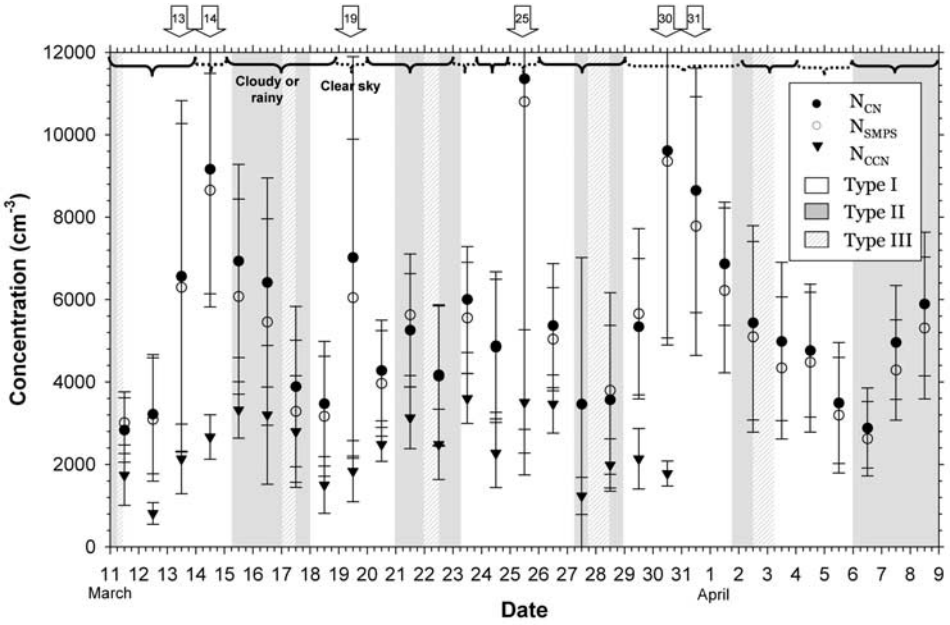

Figure 3. Variation of daily average CN, SMPS, and CCN concentrations (N_{CN}, N_{SMPS}, and N_{CCN}) during the whole measurement period. Different shadings indicate air mass types. Weather conditions for each day are marked at the top. Arrows over the top axis indicate obvious particle formation and growth event days.

CPC-3010 and SMPS-3936L10 concentrations is expected, considering the fact that aerosol concentrations are usually dominated by the Aitken mode particles (say, mostly below the SMPS upper size cut of 300 nm). The average N_{CCN} is 2463 ± 1168 cm^{-3}. This is only 43% of N_{CN} but the average N_{CCN}/N_{CN} ratio is 0.51 (Table 1, last column), which was calculated from those ratios of the corresponding 15 min average CCN and CN concentrations. This difference is due to the unavailability of CCN data after 30 March, when aerosol concentrations increased to somewhat higher values than before this date (Figure 3).

[12] When the three air mass types are compared in Table 1, type I has the highest average aerosol concentrations. However, if the time ranges are excluded when the aerosol concentrations were increased because of particle formation and growth events that occurred only during the type I air mass period (Figure 3), type II has slightly higher concentrations than type I. On the other hand, N_{CCN} is significantly higher in type II than type I regardless of the exclusion of particle formation and growth event periods. This indicates that CCN are more abundant in the air masses that originated from densely populated coastal areas and having longer residence time over the sea (type II) than those from remote continental China, Mongolia or Russia (type I). One may expect that this is in some part due to the small particles that formed by nucleation and indeed N_{CCN}/N_{CN} ratio increased slightly when particle formation and growth periods are excluded (Table 1, last column; 0.45 ± 0.17 to 0.49 ± 0.16) but this is still significantly smaller than the N_{CCN}/N_{CN} for type II. The lowest aerosol concentrations are expected for type III since the 3-d back trajectories resided almost entirely over the sea (Figure 2d). However, the contribution of sea salts may be insignificant for the Gosan submicron aerosols [*Maria et al.*, 2003].

[13] Figure 4 shows the time evolution of the SMPS measured aerosol size distributions for the whole measurement period. The six particle formation and growth event days (Figure 3) are clearly identified. There are some other days with similar but less clear behavior and they are not counted as such event days. Except for these event periods, aerosol size distributions generally do not show distinct bimodal distributions (Figure 4). This is also evident when the average SMPS size distribution for each air mass is compared (Figure 5). The type I size distribution is

Table 1. Averages of CN Concentrations (N_{CN}), SMPS Concentrations (N_{SMPS}) and Geometric Mean Diameters (D_g), CCN Concentrations (N_{CCN}), and the N_{CCN}/N_{CN} Ratios for the Entire Data Set, Type I, Type II and Type III Air Masses[a]

	N_{CN}, cm^{-3}	N_{SMPS}, cm^{-3}	D_g, nm	N_{CCN}, cm^{-3}	N_{CCN}/N_{CN}
All	5599 ± 3518	5337 ± 3406	65 ± 19	2463 ± 1168	0.51 ± 0.18
Type I	6088 ± 3988	5805 ± 3857	60 ± 18	2393 ± 1156	0.45 ± 0.17
Type I (no event)	5008 ± 2104	4771 ± 2073	63 ± 16	2295 ± 1140	0.49 ± 0.16
Type II	5231 ± 2454	4812 ± 2240	74 ± 16	2897 ± 1226	0.60 ± 0.17
Type III	3513 ± 1790	3430 ± 1750	75 ± 18	1843 ± 585	0.62 ± 0.13

[a]Averages for type I excluding particle formation and growth event periods are also shown.

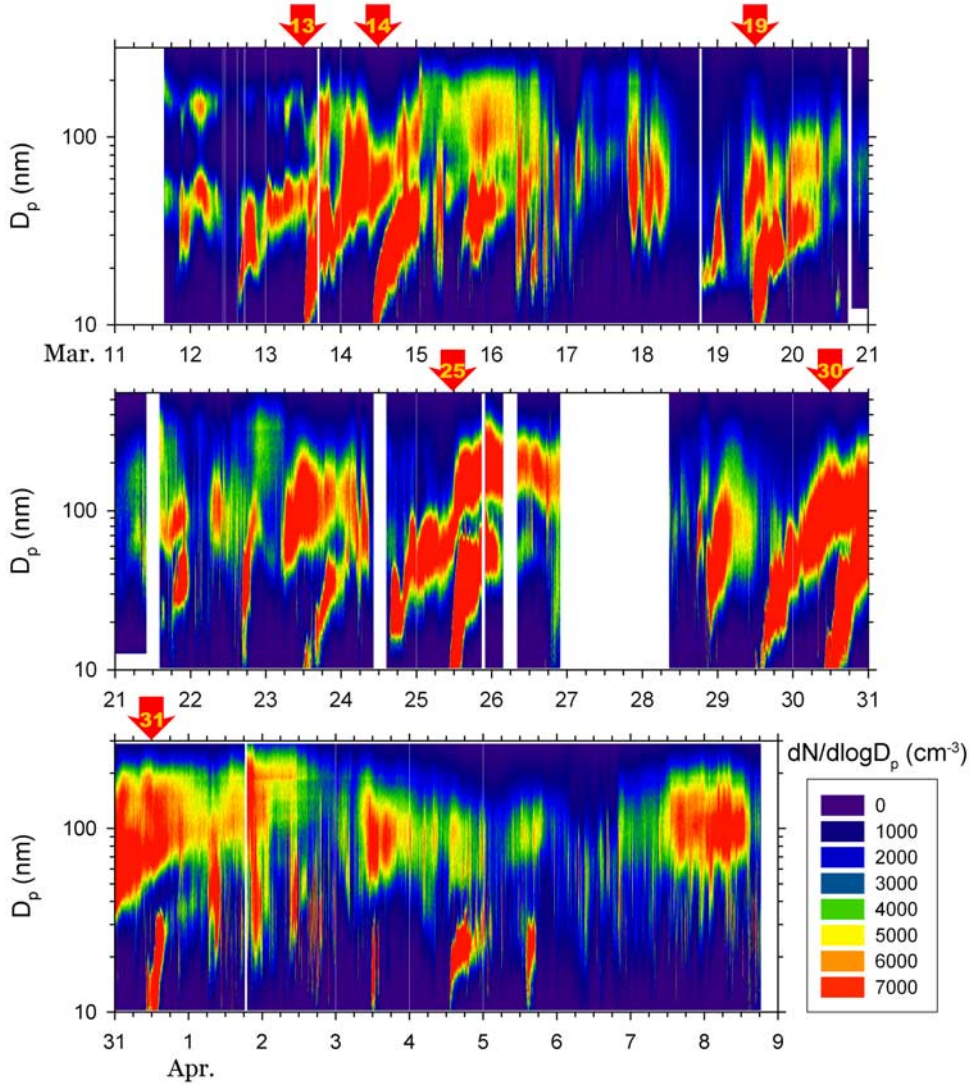

Figure 4. Time variation of SMPS size distributions for the entire measurement period. Arrows over the top axis indicate clear particle formation and growth event days.

somewhat bimodal with two modes at 35 nm and 90 nm (Figure 5a). When the influence of small particles during the six particle formation and growth event periods is excluded, the bimodal shape is still maintained but particle concentrations are reduced relatively more at smaller D_p ranges and the smaller mode D_p increases from 35 to 45 nm (Figure 5b). The type II size distribution shows a dominant mode at 100 nm (Figure 5c). The type III size distribution has one distinct mode at close to 80 nm (Figure 5d). The average geometric mean diameter (D_g) for each of the aerosol types is shown in Table 1. The smaller mode D_p of type III than type II but almost the same D_g of the two air masses indicate relatively larger proportion of larger particles for the type III size distribution because of the longer aging time for type III (Figure 2).

[14] Figure 6 shows the average diurnal variations of N_{CN}, N_{SMPS}, and N_{CCN} for the entire measurement period (Figure 6a) and when particle formation and growth event periods were excluded (Figure 6b). Early afternoon peak is conspicuous for N_{CN} and N_{SMPS} in Figure 6a because of the increase of aerosol concentrations during the particle formation and growth events that occurred on 6 d (Figure 3), which generally started near noontime and lasted for several hours to more than 10 h. The large error bars for N_{CN} in the early afternoon hours reflect the huge daily variation of concentrations associated with new particle formation. When these event periods are excluded, diurnal variations of N_{CN} and N_{SMPS} are insignificant (Figure 6b). The N_{CCN} shows negligible diurnal variation whether or not the particle formation and growth events are included (Figure 6), implying that newly formed small particles could not act as CCN because of their size limitation (more on this later). An individual particle formation and growth event day (Figure 7a) and a nonevent day (Figure 7b) are compared in Figure 7. Figure 7a shows how the particle concentrations increase and D_g suddenly falls off because of the formation of large numbers of small particles on a particle formation and growth event day, but no significant diurnal variation is obvious on a nonevent day (Figure 7b).

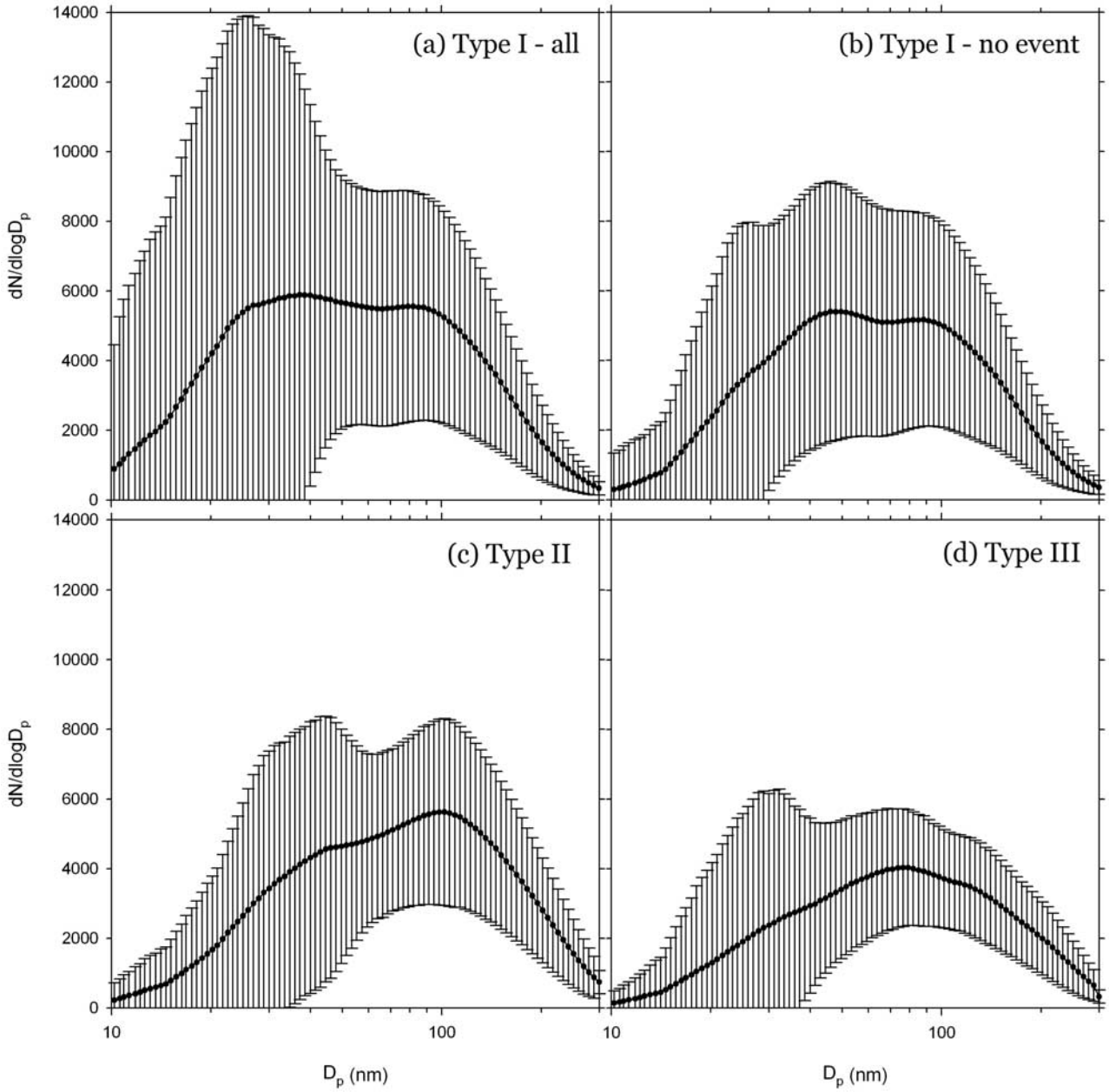

Figure 5. Air mass average SMPS size distributions for each air mass: (a) type I, (b) type I without particle formation and growth event periods, (c) type II, and (d) type III. Error bars (one standard deviation) are also shown.

Again N_{CCN} shows no significant diurnal variations on the particle formation day as well as on the nonevent day.

3.3. Particle Formation and Growth Events

[15] Figure 8 is a closer look at the diurnal variation of the SMPS measured aerosol size distributions on 14 March when a particle formation and growth event occurred. High concentrations of 10 nm particles appear at 1030 local time (LT) and the modal diameter grows as the time progresses until 0100 LT the next day. The growth curve spanning 14 h is clearly recorded. Back trajectories on this day suggest the air at Gosan surface (50 m ASL) and 500 m altitudes were coming consistently from northwest, spending the prior 24 h over the Yellow Sea. On 14 March, the measured wind at the Gosan weather station was also consistently from northwest or north with the average speed of 7 m s^{-1} until 8 PM when the wind direction changed to east or southeast. This is also the time when the growth curve is disrupted (Figure 8) but unlike the growth curve that returns to the original growth track after an hour, the wind direction never returned to northwest or north. This suggests that the event was not a local event but a regional event that occurred simultaneously in a large areal extent over the Yellow Sea. Assuming the wind speed of 7 m s^{-1}, 10 h stretches translate into 250 km distance. Indeed the SMPS measurements at the Korea Global Atmosphere

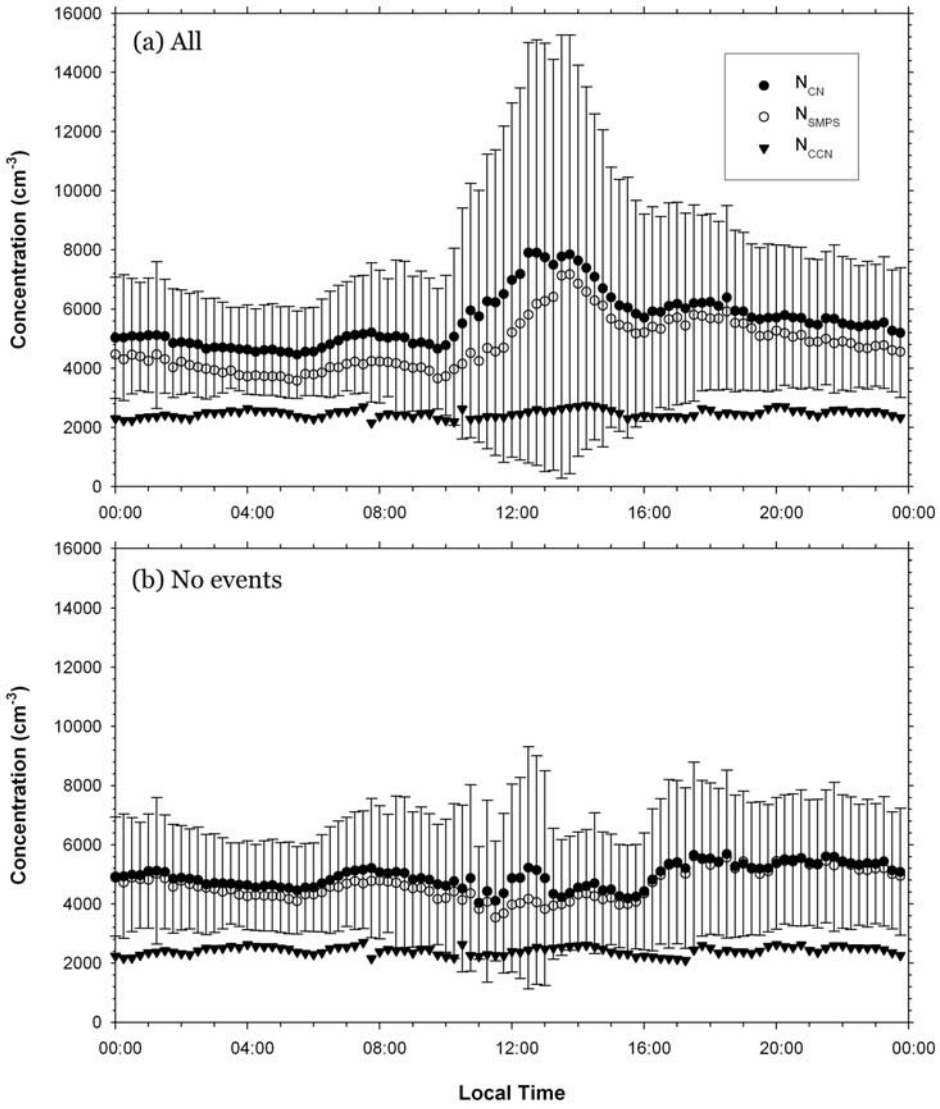

Figure 6. Average diurnal variation of CN, SMPS, and CCN concentrations (N_{CN}, N_{SMPS}, and N_{CCN}) (a) for the entire measurement period and (b) when particle formation and growth event period are excluded. Error bars (one standard deviation) for N_{CN} are also shown.

Watch Observatory (KGAWO) located at the west coast of the Korean Peninsula (~350 km north of Gosan; Figure 1) did detect almost simultaneous new particle formation and growth event on this day [*Lee et al.*, 2007]. In fact, in four out of six particle formation and growth event days at Gosan, the KGAWO also observed such events. Evidence of regional or synoptic-scale particle formation and growth events were also reported at or nearby the Gosan site during the ACE-Asia project [*McNaughton et al.*, 2004; *Buzorius et al.*, 2004]. Large-scale particle formation is also reported by *Tunved et al.* [2006] but here the particle formation occurred during the transition from maritime to continental air mass over the northern European boreal forest and the sources of precursor gases were terpenes from the boreal forest.

[16] Two upper air soundings are made every day at the Gosan weather station (0900 and 2100 LT) and therefore no vertical sounding is available in the midday. The 0900 LT sounding on this day showed a neutrally stratified atmosphere up to the temperature inversion at 1900 m ASL. As the day progressed and the surface temperature increased, possibility of vertical mixing increased. *Nilsson et al.* [2001] suggested that strong mixing during the rapid growth of boundary layer height caused an increase in the nucleation rates due to increases in the saturation ratios of precursor gases. From the measurement at Gosan during ACE-Asia, *Buzorius et al.* [2004] showed that particles were formed in upper part of the boundary layer prior to turbulent mixing by chemically driven processes and then transported down to lower altitudes as the day progressed and the mixed layer is elevated. There is no direct evidence that the particle formation and growth event on 14 March was related to either of the two explanations. The air mass back trajectories from the Gosan surface and 500 m altitude, respectively, showed almost no variation in altitude for the previous 24 h or were below 1000 ASL for more than a day

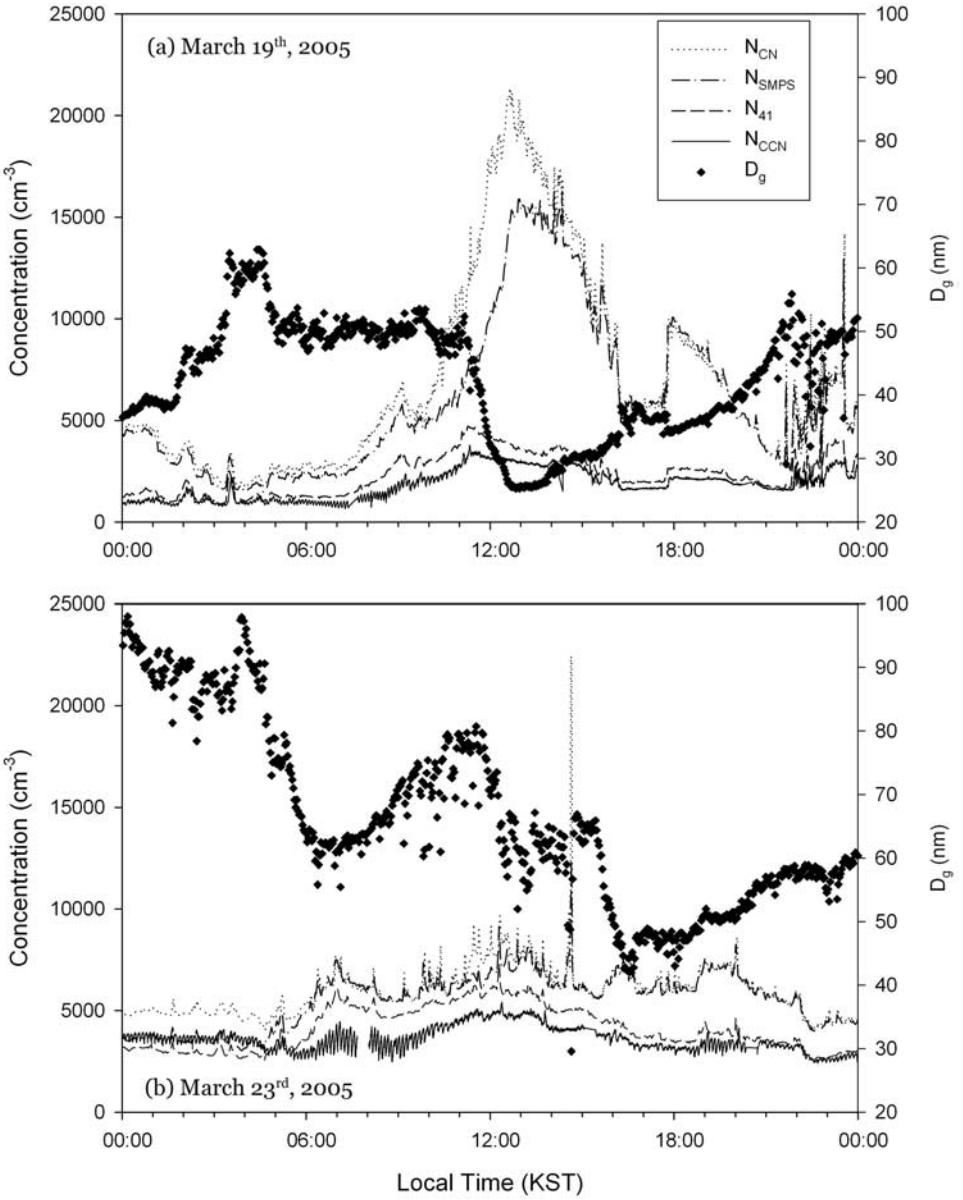

Figure 7. Diurnal variation of CN, SMPS, and CCN concentrations (N_{CN}, N_{SMPS}, and N_{CCN}) and the geometric mean diameter (D_g) for (a) a particle formation and growth day (19 March 2005) and (b) a nonevent day (23 March 2005). Also shown are the particle concentrations calculated by integrating SMPS size distributions from diameter (D_p) greater than 41 nm to the upper size limit (N_{41}).

previously, indicating that particle formation occurred near the surface altitudes. Several particle formation mechanisms in various environments have been suggested [e.g., *Kulmala et al.*, 2001, 2004; *O'Dowd et al.*, 2002] but to find the one that fits particle formations at Gosan requires detailed chemical analysis, which is out of the scope of this study.

[17] Particle formation and growth events were recorded on 5 other days (Figures 3 and 4) but the events started 1 or 2 h later and thus closer to noon than the one shown in Figure 8 and lasted for 4 to 10 h. The particle growth rate (the slope of the regression line between time and mode D_p of the aerosol size distribution) for the first 4 h for the event on 14 March (Figure 8) was 3.4 nm h^{-1} and for the other five events it ranged from 4 to 10 nm h^{-1}. These values are comparable to many of the measurements reported by *Kulmala et al.* [2001]. All six events occurred on the days that belong to type I, for which the prevailing weather conditions were clear sky (Figure 3), bringing air mostly from north or northwest directions, confirming that daytime solar radiative flux is a prerequisite for particle formation [e.g., *O'Dowd et al.*, 2002; *Lee et al.*, 2003]. Moreover, 1 or 2 d before the event, Jeju Island was usually under the influence of a frontal or low-pressure system, cleaning the air by cloud or precipitation scavenging and therefore reducing the preexisting surface areas that the precursor gases might condense onto [e.g., *McMurry et al.*, 2005]. Unlike the Mace Head coastal area observations [*O'Dowd et al.*, 2002], however, particle formation at Gosan did not

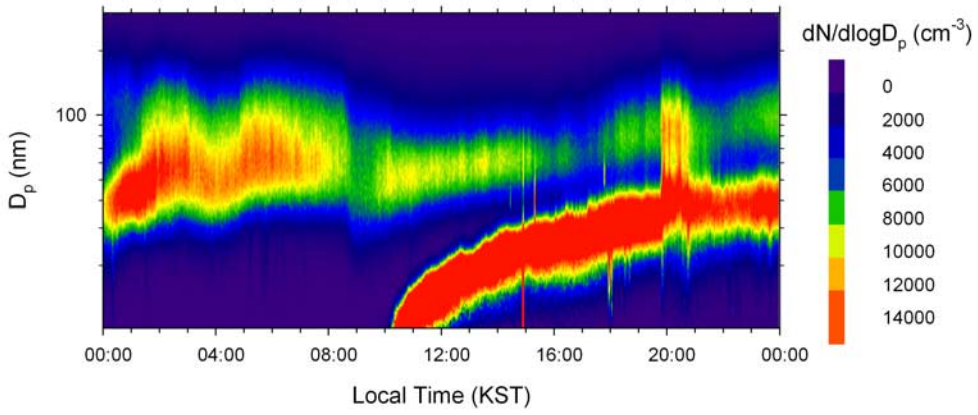

Figure 8. Detailed look at the diurnal variation of the SMPS size distributions on the day when a particle formation and growth event occurred (14 March 2005).

coincide with the occurrence of low tide (not shown) as the rugged Gosan coastline did not expose considerable amounts of marine biota during low tides. Perhaps the sample air drawn from 58 m ASL was too far from the shore to exert significant influence on the measurement. The fact that the air was coming consistently from north or northwest where no notable landmass exists for several hundred km suggests that particle formation occurred somewhere over the Yellow Sea.

3.4. CCN: Aerosol

[18] Figure 9 shows the scatterplots of N_{CN} versus N_{CCN} (Figure 9a) and N_{CN} versus N_{CCN}/N_{CN} ratio for the CCN measurement period (11–30 March 2005). The average N_{CCN}/N_{CN} ratios are listed in Table 1. There is an increasing trend of N_{CCN} with N_{CN} but the N_{CCN}/N_{CN} ratios tend to decrease as the N_{CN} increase, indicating that greater portions of aerosols are CCN inactive as CN concentration increases. It is hard to differentiate the three air mass types in Figure 9 but on average (Table 1) type I has the lowest N_{CCN}/N_{CN} and type III has slightly larger value than type II. However, N_{CCN} varies a lot for a given N_{CN}, especially for lower N_{CN} (Figure 9b). This reflects the inaccuracy of estimating CCN concentrations in polluted conditions without physical and chemical information.

[19] *Roberts et al.* [2006] and several others [e.g., *Bigg*, 1986; *Covert et al.*, 1998; *Wood et al.*, 2000; *Snider and Brenguier*, 2000] predicted CCN concentrations at a given supersaturation based on the SMPS measured aerosol size distributions. Assuming all particles are composed solely of $(NH_4)_2SO_4$, the critical dry particle diameter (D_c) can be calculated from Köhler theory [*Pruppacher and Klett*, 1997]. The D_c is 41 nm for S_c of 0.6%, the S setting of our CCN counter. This means that if ammonium sulfate is assumed for composition, only particles greater than 41 nm diameter can become CCN at 0.6% S. Integration of SMPS particle concentrations only for D_p greater than 41 nm provides predicted CCN concentration ($N_{CCN,pred}$). Figure 10 compares measured with predicted CCN concentrations based on this premise. Figure 11 plots $N_{CCN,pred}/N_{CCN}$ as a function of N_{CCN}. Overall the correspondence is very good (Figure 10a: $r^2 = 0.77$, $y = 1.13 \times +292$; Figure 11a: $N_{CCN,pred}/N_{CCN} = 1.27 \pm 0.29$). There is a tendency to overpredict for type I (Figure 11b; $N_{CCN,pred}/N_{CCN} = 1.33 \pm 0.30$) but the correspondence for type II and III are remarkable; type II has $N_{CCN,pred}/N_{CCN}$ ratio closest to one (1.10 ± 0.22) (Figure 11c) and type III has the slope of the linear regression line closest to one among all cases (1.06) (Figure 10d). Figure 7 also demonstrates that when only the particles of D_p greater than 41 nm are counted from the SMPS data, the particle concentration (N_{41}, i.e., this is equal to $N_{CCN,pred}$) follows N_{CCN} really well on the particle formation day (Figure 7a) as well as on the nonevent day (Figure 7b). The slight overprediction for type I implies somewhat less CCN active aerosols than ammonium sulfate for this air mass. Correspondingly *Maria et al.* [2003] found relatively higher fraction of organic matter (hence less soluble fraction) for the submicron aerosols of the back trajectories similar to type I than for other back trajectories. However, the good overall correspondence indicates that springtime Gosan aerosols act almost like ammonium sulfate as far as CCN activity is concerned, almost regardless of air mass origins.

[20] Another way to quantify CCN capability of aerosols is to compare experimentally determined critical diameter ($D_{c,meas}$) to that of ammonium sulfate ($D_{c,ammo}$) for a given S (e.g., 41 nm for 0.6% S from Köhler equation). The $D_{c,ammo}/D_{c,meas}$ ratio is named as a CCN activation index [*Roberts et al.*, 2006]. The integration of SMPS aerosol size distribution from the upper size limit to the D_p at which the integrated concentration equals the measured CCN concentration yields $D_{c,meas}$. The basic assumption is that particles of D_p greater than the D_c for a given S would be activated as cloud droplets and be counted as CCN by a CCN counter of the given S setting if the particle chemical composition is completely ammonium sulfate. Figure 12 plots the $D_{c,ammo}/D_{c,meas}$ ratio as a function of N_{CCN}. There seems to be no definite trend of $D_{c,ammo}/D_{c,meas}$ with N_{CCN}. A majority of the data points are in between $D_{c,ammo}/D_{c,meas}$ of 0.5 and 1.0. For type II, however, a significant fraction of the data points are above $D_{c,ammo}/D_{c,meas}$ of 1.0 line. This implies that some aerosols are even more CCN active than ammonium sulfate, i.e., particles of D_p smaller than the D_c of ammonium sulfate for the given S (0.6%) can serve as CCN, an excellent candidate being the sea salt particles such as sodium chloride. Overall the average

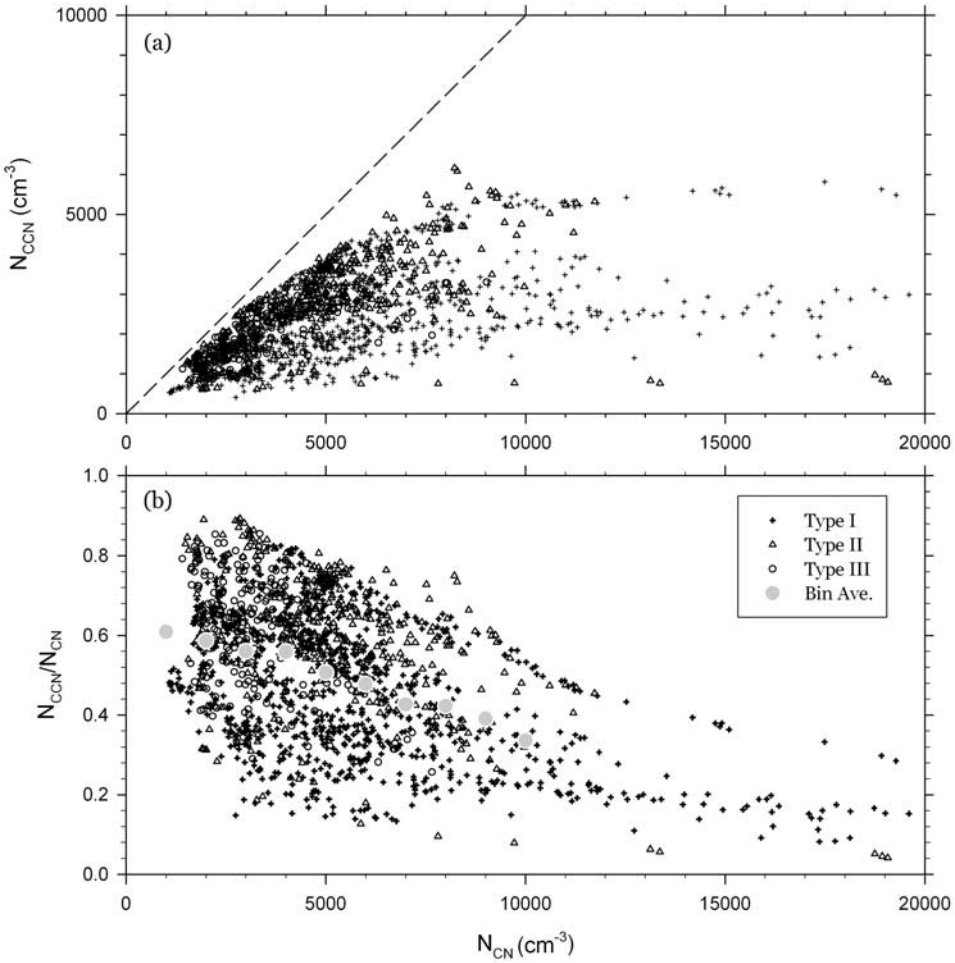

Figure 9. Scatterplots of (a) CN concentrations (N_{CN}) versus CCN concentrations (N_{CCN}) and (b) N_{CN} versus N_{CCN}/N_{CN} ratios. Gray dots in Figure 9b are 1000 cm^{-3} N_{CN} bin (1000–2000 cm^{-3}, 2000–3000 cm^{-3}, . . ., 9000–10,000 cm^{-3}) average N_{CCN}/N_{CN} ratios.

$D_{c,ammo}/D_{c,meas}$ for the entire data set is 0.79 ± 0.23 (Figure 12a).

4. Discussions

[21] CN and CCN concentrations measured at other locations are summarized in Table 2. Previous measurements in northeast Asia [*Song and Yum*, 2004; *Yum et al.*, 2005; *Kim et al.*, 2005; *Adhikari et al.*, 2005] report several thousands per cm^3 of N_{CN}. Comparable to these concentrations are the measurements at a coastal site on a remote island in eastern Mediterranean in a polluted air mass [*Eleftheriadis et al.*, 2006] or the aircraft measurements of polluted air in the eastern Pacific [*Roberts et al.*, 2006] and off the coast of Florida in continental air masses [*Hudson and Yum*, 2001]. Meanwhile *O'Dowd et al.* [2001] reported significantly low typical N_{CN} of 400–600 cm^{-3} at an eastern Atlantic coastal site in Mace Head although the concentration increased up to 7000 cm^{-3} for most polluted air. *Hoppel and Frick*'s [1990] central Pacific cruise measurements and *Hoppel et al.*'s [1990] trans-Atlantic cruise measurements reported 300 cm^{-3} or less in the central part of the oceans. Similar values were found over the Southern Ocean and northeastern Atlantic [*Bates et al.*, 2000]. Several aircraft measurements in clean marine boundary layers also reported a few hundred particles per cm^3 [*Hudson et al.*, 1998; *Yum and Hudson*, 2001, 2002, 2004; *Hudson and Yum*, 2002]. These listings suggest that the N_{CN} measured in this study (Table 1) are comparable to or greater than coastal or marine measurements with significant continental or anthropogenic influence. The N_{CN} of type III, supposedly least affected by anthropogenic influence, turns out to be about an order of magnitude higher than the background concentration in clean maritime environment. The lowest instantaneous CN concentration during the whole measurement period in this study was 979 cm^{-3} (Figure 9a), never being close to the clean maritime background concentrations listed in Table 2. However, this could very well be the background N_{CN} in the springtime northeast Asian coastal environments.

[22] Similarly to N_{CN} comparisons above, the CCN concentrations at 0.6% S measured in this study (Table 1) are comparable to some other measurements in this region [*Yum et al.*, 2005; *Adhikari et al.*, 2005] and typical continental N_{CCN} in Reno [*Hudson and Frisbie*, 1991] or northern Oklahoma [*Gasparini et al.*, 2006]. However, the average

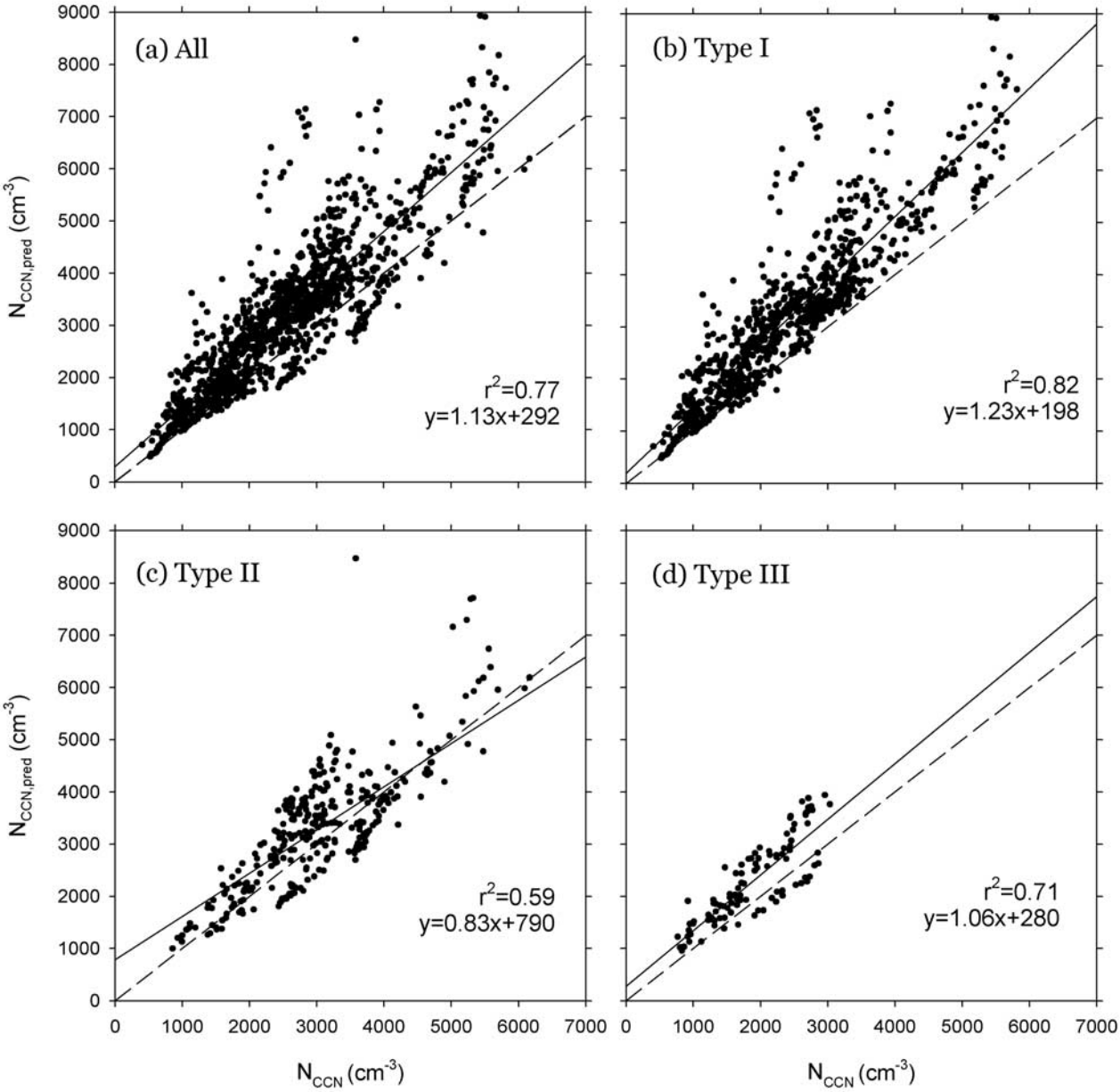

Figure 10. Scatterplots of measured CCN concentrations (N_{CCN}) versus predicted CCN concentrations ($N_{CCN,pred}$) for (a) the entire measurement period, (b) type I, (c) type II, and (d) type III. The solid lines are the linear regression lines, and the dashed lines are one to one lines.

N_{CCN} of type III (the lowest in Table 1) is an order of magnitude higher than the typical background maritime concentrations listed in Table 2 [*Jennings et al.*, 1998; *Hudson et al.*, 1998; *Chuang et al.*, 2000; *Yum and Hudson*, 2001, 2002, 2004; *Hudson and Yum*, 2002; *Roberts et al.*, 2006].

[23] Measurements in the background marine boundary layer often showed distinct bimodal aerosol size distributions with the smaller mode at $D_p \sim 40$ nm and the larger mode at ~200 nm [e.g., *Hoppel et al.*, 1990; *Hoppel and Frick*, 1990; *Bates et al.*, 2000]. The larger mode peak was often enhanced by cloud processing, the mechanism of which is fully explained by *Hoppel et al.* [1986, 1990]. Under continental influences, the aerosol size distributions in the marine environments usually showed a unimodal shape and the mode D_p varied with the aging time over the ocean from around ~80 nm for the least aged to ~250 nm for aged [e.g., *Hoppel et al.*, 1990; *Bates et al.*, 2000; *Eleftheriadis et al.*, 2006; *Roberts et al.*, 2006]. Therefore the submicron aerosol size distributions measured in this study (Figures 4 and 5) is closer to continental size distributions with a little aging time rather than the distributions that were often found in clean marine boundary layer. The type I size distribution does show bimodal nature but the smaller mode is due to the contribution from newly formed small particles and not due to a solidly established Aitken mode particles that reside in the marine air without

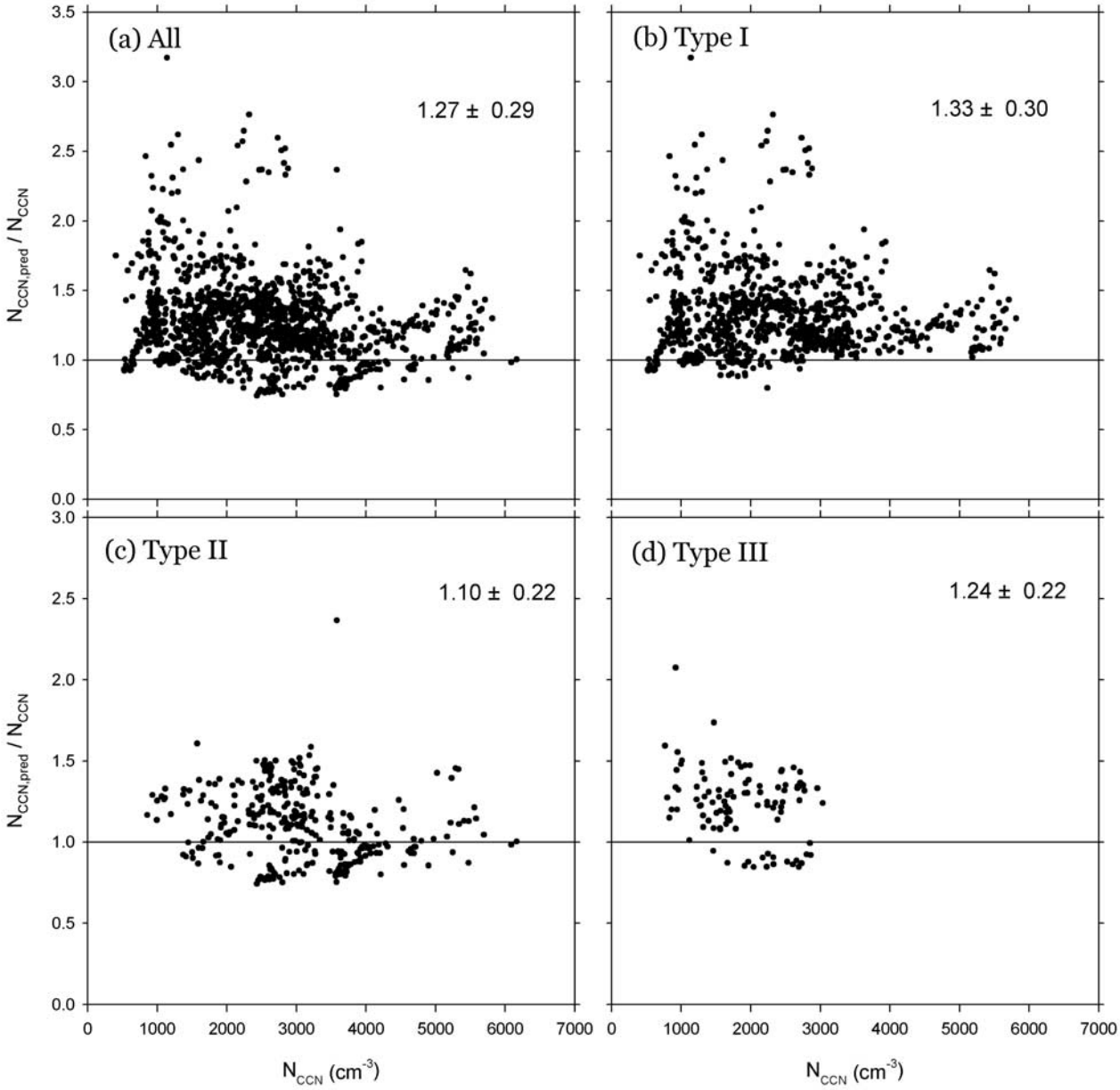

Figure 11. Predicted to measured CCN concentration ratios ($N_{CCN,pred}/N_{CCN}$) as a function of N_{CCN} for (a) the entire measurement period, (b) type I, (c) type II, and (d) type III.

changing sizes for an extended period of time (say, more than a day [*Bates et al.*, 2000]).

[24] There are reports that anthropogenically influenced air had higher N_{CCN}/N_{CN} than maritime air (Table 2): 0.41 versus 0.74 over the eastern Atlantic at 0.6% S [*Yum and Hudson*, 2002]; 0.49 versus 0.66 over the Indian Ocean at 1% S [*Hudson and Yum*, 2002]. *Adhikari et al.* [2005] also reported N_{CCN}/N_{CN} ratio of 0.3 (0.3% S) or less in the relatively clean maritime air and ~0.5 for anthropogenically influenced air. Meanwhile *Yum et al.* [2005] measured 0.64 (1.0% S) that did not vary with air mass designation. Our data seems consistent with these results: on average type II and III showed almost a factor of two differences in N_{CN} but N_{CCN}/N_{CN} were about the same (Table 1). However, this lack of trend was for relatively high aerosol concentrations. The lowest average N_{CN} given by *Yum et al.* [2005] and this study (type III) were even greater than the continental N_{CN} given by *Yum and Hudson* [2002] and *Hudson and Yum* [2002]. In fact, for N_{CN} greater than 1000 cm^{-3}, there seems to be a decreasing trend of N_{CCN}/N_{CN} with N_{CN} for individual data points (Figure 9b). The lowest N_{CCN}/N_{CN} for type I in Table 1 is expected since this air mass has remote continental origin with relatively shorter marine residence time. However, the ratio itself (0.45; Table 1) seems to be still too high for remote continental air, suggesting significant anthropogenic influence even for this air mass. *Hudson and Frisbie* [1991] observed N_{CCN}/N_{CN} ratio of 0.30 or less at 0.75% S for continental aerosols of minimal anthropogenic influence.

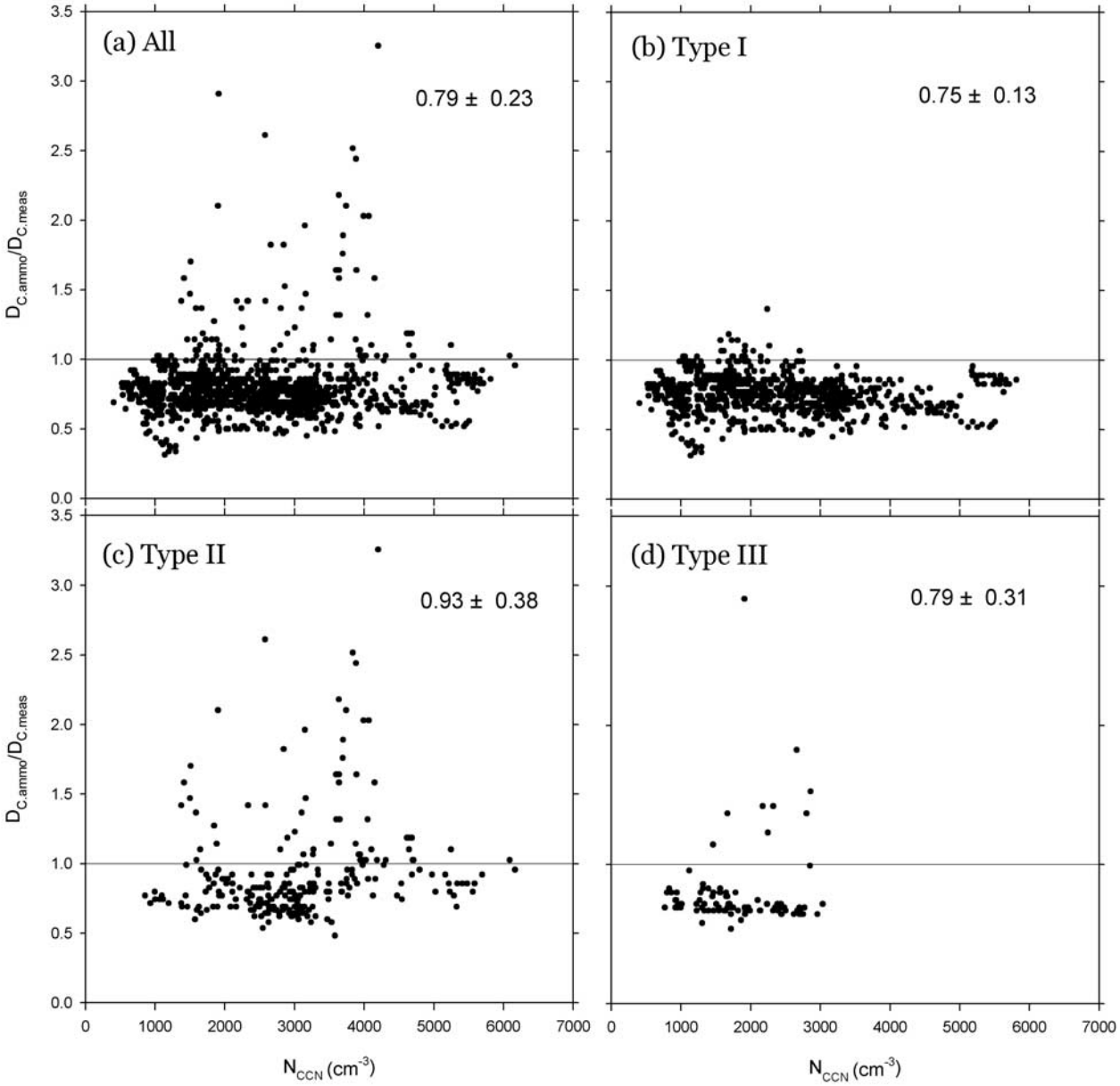

Figure 12. Critical diameter of ammonium sulfate particle at 0.6% S ($D_{c,ammo}$ = 41 nm) to the critical diameter derived from measurement ($D_{c,meas}$) by integrating SMPS aerosol size distribution from the upper size limit to the D_p at which the integrated concentration equals the measured CCN concentration for (a) the entire measurement period, (b) type I, (c) type II, and (d) type III.

[25] The predicted CCN concentrations matched very well with the measured CCN concentrations in this study (Figure 10). This is sort of a pleasant surprise for one good reason. Our method [*Roberts et al.*, 2006] uses only the size information and did not utilize size resolved aerosol chemistry information, which is essential to characterize CCN activity of aerosols, but still achieved CCN closure as good as or even better than some attempts did that utilized aerosol chemistry information [e.g., *Chuang et al.*, 2000; *Cantrell et al.*, 2000; *Roberts et al.*, 2002; *Gasparini et al.*, 2006]. This could only mean that the simple assumption of particles being composed solely of $(NH_4)_2SO_4$ is close to the reality for the springtime northeast Asian submicron aerosols almost regardless of air mass origins. Indeed *Hatakeyama et al.* [2004] found a very good correlation between sulfate and ammonium over the East China Sea and concluded that this indicated quick neutralization of sulfuric acid by ammonium in the polluted air mass. *Ishizaka and Adhikari* [2003] found that CCN compositions at a coastal site of a Japanese main island were dominated by ammonium sulfate. *McNaughton et al.* [2004] pointed out that hygroscopic growth of 25 nm particles was best explained by an ammonium sulfate/ammonium bisulfate type composition for the Gosan aerosols during ACE-Asia. However, our results are contrary to *Dusek et al.* [2006] that reported insoluble CCN than our results for the polluted air masses

Table 2. Summary of the Measurements in Comparison

Authors	Location	N_{CN}, cm^{-3}	N_{CCN}, cm^{-3}
Kim et al. [2005]	Gosan	2800–5600	
Song and Yum [2004]	Yellow Sea and the South Sea of Korea	1000 (maritime), 2000 (continental)	
	west coast of the Korean Peninsula	5000	
Yum et al. [2005]	west coast of Korean Peninsula	4000–8300	2400–5300 at 1% S
Adhikari et al. [2005]	remote southwest island of Japan	3000–5000	800–2000 at 0.3% S
Hudson and Yum [2002]	Indian Ocean	361	176 at 1% S
Hoppel and Frick [1990]	central Pacific	150–300	
Roberts et al. [2006]	eastern Pacific (pristine-anthropogenic)	<100–10000	20–350 at 0.3% S
Yum and Hudson [2002]	eastern Pacific	252–325	112–157 at 0.6% S
Hudson and Yum [2001]	off the coast of Florida	1200 (maritime), 3600 (continental)	
Hoppel et al. [1990]	American Atlantic coast, center of Atlantic, African Atlantic coast, pollution plume in Atlantic	2000, 200, 2000, 10000	
Yum and Hudson [2002]	eastern Atlantic	241–364	126–131 at 0.6% S
Chuang et al. [2000]	eastern Atlantic		27–267 at 0.1% S
O'Dowd et al. [2001]	eastern Atlantic coastal site in Mace Head	400–600 (maritime), 600–1500 (modified maritime air)	
Jennings et al. [1998]	eastern Atlantic coastal site in Mace Head		76–203 at 0.5% S (marine air), 369–1428 at 0.5% S (polluted air)
Eleftheriadis et al. [2006]	coastal site on a remote island in eastern Mediterranean	1300 (background), 3400–4000 (polluted)	
Bates et al. [2000]	Southern Ocean and northeastern Atlantic	300–500	
Yum and Hudson [2004]	Southern Ocean	260–298	32–191 at 1% S
Yum and Hudson [2001]	Artic Ocean	45–497	41–290 at 0.8% S

and are also contrary to *Hudson and Da* [1996], where the authors found that CCN solubility for the air masses under anthropogenic influences tends to be insoluble compared to cleaner air masses.

5. Conclusions

[26] Data obtained at a relatively remote coastal site at Gosan in Jeju Island, Korea during the ABC-EAREX 2005 indicates that springtime submicron aerosols were under steady continental influences, regardless of air mass designation. Even the air mass that was the closest to maritime in terms of marine residence time has the average CN and CCN concentrations an order of magnitude higher than those of clean marine boundary layer and were in fact comparable to or even higher than those of marine or coastal environments with significant continental influences.

[27] Clear sky weather conditions bringing air from northern China, Mongolia or Russia by anticyclonic circulations were found to be a prerequisite for new particle formation and growth at Gosan. Simultaneous occurrence of these events at a western coastal site in the Korean Peninsula 350 km north of Gosan suggests that these events were not local but at least regional-scale events. However, it cannot be verified if the actual formation of new particles occurred near the measurement altitude or new particles were formed aloft and then turbulent mixing took them down to the measurement altitude as the day progressed.

[28] With the assumption of particles being composed solely of ammonium sulfate, there was a very good agreement between the measured and predicted CCN concentrations based on the measured aerosol number size distributions. The air mass that has the most continental influences showed a slight tendency to overpredict CCN concentrations but the overall agreement is good enough to suggest that springtime Gosan aerosols act almost like ammonium sulfate as far as CCN activity is concerned.

[29] Lacking in this study were aerosol chemistry analyses, which will be presented by companion papers on aerosol chemistry in this special issue. Combining them with the results of this study would provide a more complete picture of springtime submicron aerosol characteristics at the coastal environment of Gosan, a suitable location to monitor background aerosol distributions in northeast Asia.

[30] **Acknowledgments.** This study is supported by the Korean Ministry of Environment as the Eco-technopia 21 project. The authors want to say special thanks to Soon-Chang Yoon of Seoul National University for allowing them to use his instrument shelter and the aerosol inlet system at the Gosan site.

References

Adhikari, M., et al. (2005), Vertical distribution of cloud condensation nuclei concentrations and their effect on microphysical properties of clouds over the sea near the southwest islands of Japan, *J. Geophys. Res.*, *110*, D10203, doi:10.1029/2004JD004758.

Albrecht, B. A. (1989), Aerosols, cloud microphysics and fractional cloudiness, *Science*, *245*, 1227–1230.

Bates, T. S., et al. (2000), Aerosol physical properties and processes in the lower marine boundary layer: A comparison of shipboard sub-micron data from ACE-1 and ACE-2, *Tellus, Ser. B.*, *52*, 258–272.

Bigg, E. K. (1986), Discrepancy between observation and prediction of concentrations of cloud condensation nuclei, *Atmos. Res.*, *20*, 81–86.

Buzorius, G., et al. (2004), Secondary aerosol formation in continental outflow conditions during ACE-Asia, *J. Geophys. Res.*, *109*, D24203, doi:10.1029/2004JD004749.

Cantrell, W., G. Shaw, C. Leck, L. Granat, and H. Cachier (2000), Relationships between cloud condensation nuclei spectra and aerosol particles on a south-north transect of the Indian Ocean, *J. Geophys. Res.*, *105*(D12), 15,313–15,320.

Chuang, P. Y., et al. (2000), CCN measurements during ACE-2 and their relationship to cloud microphysical properties, *Tellus, Ser. B*, *52*, 843–867.

Covert, D. S., J. L. Gras, A. Wiedensohler, and F. Stratmann (1998), Comparison of directly measured CCN with CCN modeled from the number size distribution in the marine boundary layer during ACE 1 at Cape Grim, Tasmania, *J. Geophys. Res.*, *103*(D13), 16,597–16,608.

Draxler, R. R., and G. D. Hess (1998), An overview of the HYSPLIT4 modeling system for trajectories, dispersion and deposition, *Aust. Meteorol. Mag.*, *47*, 295–308.

Dusek, U., et al. (2006), Size matters more than chemistry for cloud-nucleating ability of aerosol particles, *Science*, *312*, 1375–1378.

Eleftheriadis, K., et al. (2006), Size distribution, composition and origin of the submicron aerosol in the marine boundary layer during the eastern Mediterranean "SUB-AERO" experiment, *Atmos. Environ.*, *40*, 6245–6260.

Gasparini, R., D. R. Collins, E. Andrews, P. J. Sheridan, J. A. Ogren, and J. G. Hudson (2006), Coupling aerosol size distributions and size-resolved hygroscopicity to predict humidity-dependent optical properties and cloud condensation nuclei spectra, *J. Geophys. Res.*, *111*, D05S13, doi:10.1029/2005JD006092.

Harshvardhan, G. (1993), Aerosol-climate interactions, in *Aerosol-Cloud-Climate Interactions*, edited by P. V. Hobbs, pp. 76–96, Elsevier, New York.

Hatakeyama, S., A. Takami, F. Sakamaki, H. Mukai, N. Sugimoto, A. Shimizu, and H. Bandow (2004), Aerial measurement of air pollutants and aerosols during 20–22 March 2001 over the East China Sea, *J. Geophys. Res.*, *109*, D13304, doi:10.1029/2003JD004271.

Hobbs, P. V. (2000), *Introduction to Atmospheric Chemistry*, 262 pp., Cambridge Univ. Press, New York.

Hoppel, W. A., and G. M. Frick (1990), Submicron aerosol size distributions measured over the tropical and South Pacific, *Atmos. Environ., Part A*, *24*, 645–659.

Hoppel, W. A., G. M. Frick, and R. E. Larson (1986), Effect of nonprecipitation clouds on the aerosol size distribution in the marine boundary layer, *Geophys. Res. Lett.*, *13*, 125–128.

Hoppel, W. A., J. W. Fitzgerald, G. M. Frick, and R. E. Larson (1990), Aerosol size distributions and optical properties found in the marine boundary layer over the Atlantic Ocean, *J. Geophys. Res.*, *95*, 3659–3686.

Hudson, J. G., and X. Da (1996), Volatility and size of cloud condensation nuclei, *J. Geophys. Res.*, *101*, 4435–4442.

Hudson, J. G., and P. R. Frisbie (1991), Surface cloud condensation nuclei and condensation nuclei measurements at Reno, Nevada, *Atmos. Environ., Part A*, *25*, 2285–2299.

Hudson, J. G., and S. S. Yum (2001), Maritime/continental drizzle contrasts in small cumuli, *J. Atmos. Sci.*, *58*, 915–926.

Hudson, J. G., and S. S. Yum (2002), Cloud condensation nuclei spectra and polluted and clean clouds over the Indian Ocean, *J. Geophys. Res.*, *107*(D19), 8022, doi:10.1029/2001JD000829.

Hudson, J. G., Y. Xie, and S. S. Yum (1998), Vertical distributions of cloud condensation nuclei spectra over the summertime Southern Ocean, *J. Geophys. Res.*, *103*, 16,609–16,624.

Huebert, B. J., et al. (2003), An overview of ACE-Asia: Strategies for quantifying the relationships between Asian aerosols and their climatic impacts, *J. Geophys. Res.*, *108*(D23), 8633, doi:10.1029/2003JD003550.

Intergovernmental Panel on Climate Change (2001), *Climate Change 2001: The Scientific Basis: Contribution of Working Group I to the Third Assessment Report of the Intergovernmental Panel on Climate Change*, edited by J. T. Houghton et al., 881 pp., Cambridge Univ. Press, New York.

Ishizaka, Y., and M. Adhikari (2003), Composition of cloud condensation nuclei, *J. Geophys. Res.*, *108*(D4), 4138, doi:10.1029/2002JD002085.

Jaenicke, R. (1993), Tropospheric aerosols, in *Aerosol-Cloud-Climate Interactions*, edited by P. V. Hobbs, pp. 1–32, Elsevier, New York.

Jennings, S. G., M. Geever, and T. C. O'Connor (1998), Coastal CCN measurements at Mace Head with enhanced concentrations in strong winds, *Atmos. Res.*, *46*, 243–252.

Kim, J., S.-C. Yoon, A. Jefferson, W. Zahorowski, and C.-H. Kang (2005), Air mass characterization and source region analysis for the Gosan super-site, Korea, during the ACE-Asia 2001 field campaign, *Atmos. Environ.*, *39*, 6513–6523.

Kim, Y. P., et al. (1998), Monitoring of air pollutants at Kosan, Cheju Island, Korea, during March–April 1994, *J. Appl. Meteorol.*, *37*, 1117–1126.

Kulmala, M., et al. (2001), Overview of the international project on biogenic aerosol formation in the boreal forest (Biofor), *Tellus, Ser. B*, *53*, 324–343.

Kulmala, M., et al. (2004), Formation and growth rates of ultrafine atmospheric particles: A review of observations, *J. Aerosol Sci.*, *35*, 143–176.

Lee, S. H., et al. (2003), Particle formation by ion nucleation in the upper troposphere and lower stratosphere, *Science*, *301*, 1886–1889.

Lee, Y.-G., B.-C. Choi, and S. S. Yum (2007), Characteristics of atmospheric aerosols observed at Anmyeon, Korea, during the ABC Gosan EAREX 2005 campaign period, *Int. J. Appl. Environ. Sci*., in press.

Maria, S. F., et al. (2003), Source signatures of carbon monoxide and organic functional groups in Asian Pacific Regional Aerosol Characterization Experiment (ACE-Asia) submicron aerosol types, *J. Geophys. Res.*, *108*(D23), 8637, doi:10.1029/2003JD003703.

McNaughton, C. S., et al. (2004), Spatial distribution and size evolution of particles in Asian outflow: Significance of primary and secondary aerosols during ACE-Asia and TRACE-P, *J. Geophys. Res.*, *109*, D19S06, doi:10.1029/2003JD003528.

McMurry, P. H., et al. (2005), A criterion for new particle formation in the sulfur-rich Atlantic atmosphere, *J. Geophys. Res.*, *110*, D22S02, doi:10.1029/2005JD005901.

Nilsson, E. D., U. Rannik, M. Kulmala, G. Buzorius, and C. D. O'Dowd (2001), Effects of continental boundary layer evolution, convection, turbulence and entrainment on aerosol, *Tellus, Ser. B*, *53*, 441–461.

O'Dowd, C. D., E. Becker, and M. Kulmala (2001), Mid-latitude North Atlantic aerosol characteristics in clean and polluted air, *Atmos. Res.*, *58*, 167–185.

O'Dowd, C. D., et al. (2002), A dedicated study of new particle formation and fate in the coastal environment (PARFORCE): Overview of objectives and achievements, *J. Geophys. Res.*, *107*(D19), 8108, doi:10.1029/2001JD000555.

Pruppacher, H. R., and J. D. Klett (1997), *Microphysics of Clouds and Precipitation*, 954 pp., Springer, New York.

Ramanathan, V., et al. (2001), Indian Ocean Experiment: An integrated analysis of the climate forcing and effects of the great Indo-Asian haze, *J. Geophys. Res.*, *106*(D22), 28,371–28,398.

Roberts, G., and A. Nenes (2005), A continuous-flow stream-wise thermal gradient CCN chamber for atmospheric measurements, *Aerosol Sci. Technol.*, *39*, 206–221.

Roberts, G., P. Artaxo, J. Zhou, E. Swietlicki, and M. O. Andrea (2002), Sensitivity of CCN spectra on chemical and physical properties of aerosol: A case study from the Amazon Basin, *J. Geophys. Res.*, *107*(D20), 8070, doi:10.1029/2001JD000583.

Roberts, G., G. Mauger, O. Hadley, and V. Ramanathan (2006), North American and Asian aerosols over the eastern Pacific Ocean and their role in regulating cloud condensation nuclei, *J. Geophys. Res.*, *111*, D13205, doi:10.1029/2005JD006661.

Seinfeld, J. H., and S. N. Pandis (1998), *Atmospheric Chemistry and Physics*, 1326 pp., John Wiley, Hoboken, N. J.

Snider, J., and J. Brenguier (2000), Cloud condensation nuclei and cloud droplet measurements during ACE-2, *Tellus, Ser. B*, *52*, 828–842.

Song, K. Y., and S. S. Yum (2004), Maritime-continental contrasts of cloud microphysics during ACE-Asia, *J. Korean Meteorol. Soc.*, *40*, 177–189.

Tunved, P., et al. (2006), High natural aerosol loading over boreal forests, *Science*, *312*, 261–263.

Twomey, S. (1977), The influence of pollution on the shortwave albedo of clouds, *J. Atmos. Sci.*, *34*, 1149–1152.

Wood, R., et al. (2000), Boundary layer and aerosol evolution during the third Lagrangian experiment of ACE-2, *Tellus, Ser. B*, *52*, 401–422.

Yum, S. S., and J. G. Hudson (2001), Vertical distributions of cloud condensation nuclei spectra over the springtime Arctic Ocean, *J. Geophys. Res.*, *106*, 15,045–15,052.

Yum, S. S., and J. G. Hudson (2002), Maritime/continental microphysical contrasts in stratus, *Tellus, Ser. B*, *54*, 61–73.

Yum, S. S., and J. G. Hudson (2004), Wintertime/summertime contrasts of cloud condensation nuclei and cloud microphysics over the Southern Ocean, *J. Geophys. Res.*, *109*, D06204, doi:10.1029/2003JD003864.

Yum, S. S., J. G. Hudson, K. Y. Song, and B.-C. Choi (2005), Springtime cloud condensation nuclei concentrations on the west coast of Korea, *Geophys. Res. Lett.*, *32*, L09814, doi:10.1029/2005GL022641.

D. Kim and G. Roberts, Center for Atmospheric Sciences, Scripps Institution of Oceanography, La Jolla, CA 92093, USA.

J. H. Kim, K. Song, and S. S. Yum, Department of Atmospheric Sciences, Yonsei University, Seoul 120-749, South Korea. (ssyum@yonsei.ac.kr)